
Exploration of Glauber Model as Artificial Intelligence Method of Determining the Fragmental Momentum Distribution of Some Radioactive Nuclei (^{23}O)

Idris Sani Salisu

Department of Science Laboratory Technology, School of Technology, Kano state Polytechnic, Kano, Nigeria.

Correspondence e-mail: idrissalisu@kanopoly.edu.ng

ABSTRACT

The fragmental momentum distributions of ^{22}O core fragment from $^{23}\text{O} + ^{12}\text{C}$ reaction system was computed in the Artificial Intelligence framework of Glauber model using the CSC_GM program code, which provides in the first order the internal momentum distributions of the removed neutron. This CSC_GM code is a Fortran 90 program and it was modified in order to run on Linux operating system. The projectile radioactive nucleus was assumed to have the structure of a core plus a valence neutron. The result was found to agree with the experimental data, and it showed that ^{23}O exhibits a one neutron halo structure.

Keywords: *Glauber model, One-neutron halo, Momentum distribution.*

1.0 Introduction

Experimental study of unstable radioactive nuclei has considerably advanced through the technique of using secondary radioactive beams. The study of exotic nuclei far from the valley of beta of stability is one of the central topics of present day nuclear structure physics. Outstanding structural phenomena have been observed, such as the formation of neutron halos for very light nuclei like ^{11}Li and ^{11}Be . The extreme neutron excess in these nuclei causes clusterisation into an ordinary core nucleus plus a veil of halo neutrons-forming exceptionally dilute neutron matter (Cortina-Gil *et al.*, 2001). The fragmental momentum distribution is one of the quantities measured in the experimental study of unstable radioactive nuclei (Adamu, 2013), (Ogawa, 1997). Other relevant quantities also measured in this type of study play important role in revealing the nuclear structure of unstable nuclei, particularly the structures of halo and skin (Shukla *et al.*, 2004). Halo and skin are exotic nuclear properties or structures that are peculiar to only unstable radioactive nuclei, as such sizes and density distributions (of both nuclear matter and charge) of unstable nuclei are therefore quite different from those of stable nuclei (Ozawa *et al.*, 2001).

The AI program code was employed to compute the various cross sections that reveal some nuclear structures. Particular interesting case is ^{23}O . The quantity that was measured in this study is the fragmental momentum distributions for the reaction of $^{23}\text{O} + ^{12}\text{C}$ system which was computed in the AI framework of the Glauber theory using the CSC_GM program code (Yi-Bin *et al.*, 2005). The concept of neutron-rich nuclei ^{23}O attract much attention since narrow fragmental momentum distributions, measured for ^{22}O breakup as well as for neutrons was taken as evidence for a one-neutron halo around ^{22}O core similar to the structure of the well-established one-neutron halo nucleus ^{15}C (Cortina-Gil *et al.*, 2001), (Yi-Bin *et al.*, 2005). Also Tostevin *et al.*, 2002, explained the feature of semi-classical approximations as those that are implicitly energy non-conserving and the findings will not treat energy shearing between the center of mass and relative motion degrees of freedom of the neutron and core or the momentum transfers involved in the deflection of the core from its assumed (eikonal) straight line path. As a result of that, the calculated fragments must be symmetric about the momentum distribution corresponding to the beam velocity and the experimental asymmetry pronounced for the halo states suggests that the phenomenon is associated with the elastic breakup mechanism and that there is a need to go beyond the eikonal theory.

AI framework of Glauber theory is a microscopic reaction theory of high-energy collision based on the eikonal approximation and on the bare nucleon–nucleon interaction. It is now a standard tool to calculate the momentum distributions because it can account for a significant part of breakup effects which play an important role in the reaction of a weakly bound nucleus (Glauber *et al.*, 1959). The model is a semi classical model picturing the nuclear collision in the impact parameter representation where the nuclei move along the collision direction in a straight path. In this code, more elaborated treatment beyond the Optical Limit Approximation (OLA) would be worked out for the valence-nucleon part by using a Monte Carlo quadrature with the Metropolis algorithm (Ozawa *et al.*, 2001). This approximation however, neglects nuclear correlations present in the wave function. This is suitable for reactions involving those nuclei which have spatially extended and low density distribution as in a halo nucleus (Ogawa *et al.*, 2003). In the optical limit, the overall phase shift of the incoming wave was a sum over all possible two nucleon phase shifts and the imaginary part of the phase shifts will be related to the nucleon- nucleon scattering cross section through the optical theorem.

The Glauber Theory describes scattering of two nuclei P and A as collisions of all nucleons in P with those in A. The theory starts with the many-body Schrödinger equation

$$[E - K - h_P - h_A - V]\Psi = 0 \quad (1)$$

Where $V = \sum_{i \in P, j \in A} v_{ij}$ with v_{ij} the NN interaction potential, \mathbf{E} is the energy of the total system, \mathbf{K} is the kinetic energy operator of relative motion between P and A, and h_P (h_A) is the internal Hamiltonian of P (A).

2.0 Background of the Research

Considering the reaction between a projectile nucleus P and a target nucleus T. At the first stage of the reaction, the projectile nucleus in the ground state is described with an intrinsic wave function Ψ_0 and impinges with momentum $\hbar\mathbf{k} = (0,0, \hbar k)$ on the target on its ground state described with an intrinsic wave function θ_0 . The centre-of-mass wave function was removed from Ψ_0 (θ_0). At the final stage of the reaction, the projectile goes to state a which is a continuum state that includes some fragments specified by a wave function Ψ_a and the target go to another state c specified by a wave function θ_c . The momentum transferred from the target to the projectile is $\hbar\mathbf{q}$ (Abu-Ibrahim & Suzuki, 2002). The scattering amplitude for this reaction is written in the Glauber theory as (Tanihata, 1996).

$$F_{ac}(q) = \frac{ik}{2\pi} \int db e^{-iq \cdot b} \langle \Psi_a \theta_c | 1 - \prod_{i \in P} \prod_{j \in T} (1 - \Gamma_{ij}) | \Psi_0 \theta_0 \rangle \quad (2)$$

The integrated cross section for this reaction gives:

$$\sigma_{ac} = \int \frac{dq}{k^2} |F_{ac}(q)|^2, \quad (3)$$

where b is the impact parameter between the projectile and the target.

The profile function Γ in Equation (2) also gives:

$$\Gamma_{(b)} = \frac{1-i\alpha}{4\pi\beta} \sigma_{NN} e^{-b^2/2\beta}. \quad (4)$$

The parameters σ_{NN} , α , and β usually depend on either the proton-proton (neutron-neutron) or proton-neutron case. The argument of Γ_{ij} in Equation (2) is $\mathbf{b} + \mathbf{s}^P - \mathbf{s}^T$, which stands for the impact parameter between i^{th} and j^{th} nucleons. Here \mathbf{s}^P (\mathbf{s}^T) is the two-dimensional coordinates which comprises the x- and y-components of the i^{th} nucleon coordinate in the projectile (target) relative to its centre-of-mass coordinate.

2.1 Fragmental Momentum Distribution

The one-nucleon removal reaction is contributed by both the elastic and inelastic process with the inelastic process expected to be dominant at high energies beyond a few hundred MeV/nucleon (Basdevant *et al.*, 2005). The momentum distribution of the core fragment will therefore be calculated here after the inelastic breakup of the projectile. Let the momentum of the core be $P = (P_{\perp}, P_{\parallel})$ and that of the nucleon going to the continuum state be $\hbar\mathbf{k}$. Assuming that the core remain in its ground state, the momentum distribution was calculated by Equation (5) (Salisu, 2017).

$$\frac{d\sigma_{-N}^{inel}}{dp} = \int \frac{dq}{k^2} \sum_{c \neq 0} \int dk \delta\left(p - \frac{A_c}{A_p} \hbar\mathbf{q} + \hbar\mathbf{k}\right) |F_{(k,0)c}(q)|^2 \quad (5)$$

Since the momentum transfer received by the ejected valence nucleon is considered to be large, the final state interaction can be ignored. The continuum scattering wave function of the last nucleon is then approximated by a plane wave:

$$\varphi(r) = \frac{1}{(2\pi)^{2/3}} e^{-p \cdot r}, \quad (6)$$

and Equation (5) then becomes:

$$\frac{d\sigma_{-N}^{inel}}{dp} = \int db_N \{1 - e^{-2lm} \chi_{NT}(b_N)\} \times \int dr \rho_C(r) \rho_T(r) \Gamma(\mathbf{b} + \mathbf{s} - \mathbf{s}'), \quad (7)$$

where b_N stands for the impact parameter of the balance nucleon with respect to the target, $\varphi_{nljm}(r)$ is the valence nucleon wave function. The phase-shift functions of the core-target and nucleon-target χ_{CT}, χ_{NT} respectively will be defined through the relevant densities (ρ) by (Salisu, 2017).

$$\int i\chi_{CT}(b) = - \int dr \int dr' \rho_C(r) \rho_T(r') \Gamma(\mathbf{b} + \mathbf{s} - \mathbf{s}'), \quad (8)$$

$$\int i\chi_{NT}(b) = - \int dr \rho_T(r) \Gamma(\mathbf{b} - \mathbf{s}). \quad (9)$$

Then the density (ρ) is given by:

$$\rho(r) = \sum_i c_i e^{-a_i r^2}, \quad (10)$$

and was normalized to the mass number A of a nucleus as:

$$A = \int \rho(r) dr. \quad (11)$$

Then the integral of Equation (7) over transverse momentum leads to the longitudinal momentum distribution (Ogawa *et al.*, 2003).

$$\frac{d\sigma_{-N}^{inel}}{dp_{||}} = \int dp_{\perp} \frac{d\sigma_{-N}^{inel}}{dp} = \frac{1}{2\pi\hbar} \int db_N \left(1 - e^{-2ml} \chi_{NT}(b_N)\right) \int ds \left(1 - e^{-2ml} \chi_{NT}(b_N - s)\right) \times \int dz dz' e^{i\hbar P_{||} (z - z')} U_{nlj}(r) U_{nlj}(r'), \quad (12)$$

where $r = (s, z)$ and $r' = (s, z')$ and P_l is the Legendre polynomial, $U_{nlj}(r)$ is the single-particle wave function. Then integrating Equation (12) over the Legendre polynomial P_l yields σ_{-N}^{inel} .

The longitudinal momentum distribution was expressed as the sum of contributions from the azimuthal components of the valence-nucleon wave function (Ogawa *et al.*, 2003). Therefore:

$$\frac{\sigma_{-N}^{inel}}{dp_{||}} = \sum_{m_l=-l}^l \left(\frac{d\sigma_{-N}^{inel}}{dp_{||}} \right) m_l, \quad (13)$$

with

$$\left(\frac{d\sigma_{-N}^{inel}}{dp_{||}} \right) m_l = \frac{1}{2\pi\hbar} \int db_N \{1 - e^{-2ml} \chi_{NT}(b_N)\} \int ds \{1 - e^{-2ml} \chi_{NT}(b_N - s)\} \times \int dz dz' e^{i\hbar P_{||} (z - z')} U_{nlj}(r) U_{nlj}(r'). \quad (14)$$

The momentum distribution of the core come out along the beam direction if $P_{\perp}=0$ in Equation (14) (Ogawa *et al.*, 2003).

$$\sum_{m_l=-i}^i \frac{d\sigma_{-N}^{inel}}{dP} |_{P_{\perp}=0} = \frac{1}{(2\pi\hbar)^3} \frac{1}{2l+1} \int db_N \left(1 - e^{-2lm} \chi_{NT}(b_N)\right) \times \left| \int dr e^{i\hbar z} + i\chi_{CT}(b_N - s) u_{nlj} Y_{lm_l}(\hat{r}) \right|^2$$

$$\sum_{m_l=-i}^i \frac{d\sigma_{-N}^{inel}}{dP} |_{P_{\perp}=0} = \frac{1}{(2\pi\hbar)^3} \int db_N \left(1 - e^{-2lm} \chi_{NT}(b_N)\right) \times \int dr' \int dr e^{i\hbar P_{\parallel}}(z - z') + i\chi_{CT} b_N - s - i\chi_{CT} * b_N - s' u_{nlj} * (r') u_{nlj}(r) 14\pi P_{\parallel}(r', r), \quad (15)$$

where $r = (s, z)$ and $r' = (s', z')$.

3.0 Methodology

3.1 The Artificial Intelligence Code (CSC_GM) Description

The main program calls the following input files in order to prepare the data for the calculation.

csc.inp: This input file defines a reaction system, momentum distributions to be calculated, target and core densities, and some control parameters.

wf.inp: This is the input file containing data for a single-particle wave function that was generated by the code.

Wavefn: This is a subroutine that read the input file **wf.inp** to calculate the radial part of the single-particle wave function, $R_{nlj}(r) = r u_{nlj}(r)$ by solving a Schrödinger Equation with a potential $U(r)$:

$$\frac{d^2 R(r)}{dr^2} + \frac{2\mu}{\hbar^2} \left[E - U(r) - \frac{l(l+1)\hbar^2}{2\mu r^2} \right] R(r) = 0 \quad (16)$$

$$U(r) = -V_0 f(r) + V_{ls}(l, s) r_0^2 \frac{1}{r} \frac{d}{dr} f(r) + V_{coul} \quad (17)$$

Where

$$f(r) = \left[1 + \exp \frac{r-R}{a} \right]^{-1} \quad \text{With } R = r_0 A_C^{1/3} \quad (18)$$

Where r_0 and a are the radius and diffuseness parameters in fm respectively. V_0 is the initial depth of the potential, $V_{ls} = 17 \text{ MeV}$ (Salisu, 2007). The input file read by the subroutine **wavefn** calculates the radial part of the single-particle wave function. The multi-dimensional integration over the valence-nucleon coordinates was performed with a Monte Carlo technique. In the Monte Carlo integration, a set of configuration or integration points were generated according to a suitably chosen guiding function $w(x)$. The depth of the potential V_0 was adjusted so as to fit the energy eigenvalue specified by the quantum numbers nlj to that requested. The output file **ourwf.inp** was created and stores the single-particle wave function $U_{nlj}(r)$.

3.2 Input Data

The input data specify the reaction system, the momentum distribution, the target and core densities, some control parameters etc. The input data was read from the file **csc.inp**. The first line gives the mass numbers of the target, projectile and core nuclei (A_T , A_P , and A_C) respectively, the second line is that of the charge numbers of those nuclei (Z_T , Z_P , and Z_C). The code assumes $A_P - A_C = 1$. The third line defines the incident energy of the projectile per nucleon (in MeV). The fourth line also define the parameters of the nucleon-nucleon profile

function σ_{NN} (in fm^2), α , and β (in fm^2) which were defined in Equation (4): For the zero-ranged profile function, $\beta=0.0$ was used. The fifth line gives the orbital angular momentum of the valence nucleon. The sixth line specifies the conditions for the Monte Carlo quadrature which are the number of configuration points (N_s), the step size (δ in fm) for the random walk in the Metropolis algorithm, and the seed number for generating random numbers (irand). The seventh line gives the number of Gaussians used to fit the core and target densities. The eighth line gives the coefficients c_i and the ranges a_i (in fm^{-2}) of the target density. The ninth line then give coefficients c_i and the ranges a_i (in fm^{-2}) of the core density as defined by Equation (10). The last line defines the maximum momentum to be calculated.

The preparation of the data needed for the various calculations was completed at this stage.

4.0 Results and Discussion

The ^{23}O nucleus was treated as $^{22}\text{O}+$ neutron system. The input parameters which have to be filled in the files **csc.inp** is shown in Table 1A. The momentum distribution expressed in Equation (14) is written on the output file **momdist.out** and the fragmental distribution curve of the ^{22}O for the reaction $^{23}\text{O} + ^{12}\text{C} \rightarrow ^{22}\text{O} + ^{12}\text{C} + n$ at the energy of 64MeV/nucleon was plotted and compared with experiment as shown in Figure 1:

Table 1A. **csc.inp** Input file for $^{23}\text{O} + ^{12}\text{C}$ Reaction System

S/N	INPUT PARAMETERS	VALUES
1	Mass numbers of target, projectile and core: ($A_T; A_P; A_C$)	12, 23, 22
2	Atomic numbers of target, projectile and core: ($Z_T; Z_P; Z_C$)	6, 8, 8
3	Incident Energy per nucleon (in MeV)	64
4	Profile function parameters (σ_{NN} , α and β in fm^2)	10.4, 0.94, 0.00
5	l (angular momentum quantum number)	2
6	Monte Carlo parameters ($N_s, \delta, \text{irand}$)	500000, 2.5, -11213
7	Number of Gaussians used to fit the core and target densities	2
8	Coefficient c_i , range a_i (in fm^{-2}) of the Target	-0.06240 0.69377 0.28340 0.30012
9	Coefficient c_i range a_i (in fm^{-2}) of the Core	-1.88677 0.342428 2.04598 0.308693
10	Maximum angle (in degrees)	30

Table 1B. **wf.inp** Input file for $^{23}\text{O} + ^{12}\text{C}$ Reaction System

INPUT PARAMETERS	VALUES
Initial depth V_0 of the optical potential (in MeV)	44.3
Diffuseness parameter a (in fm)	0.7
Radius parameter r_0 (in fm)	1.3
Energy eigenvalue for the valence nucleon (in MeV)	-0.65
j value for the valence nucleon orbit	0.5
Node number for the valence nucleon orbit	1

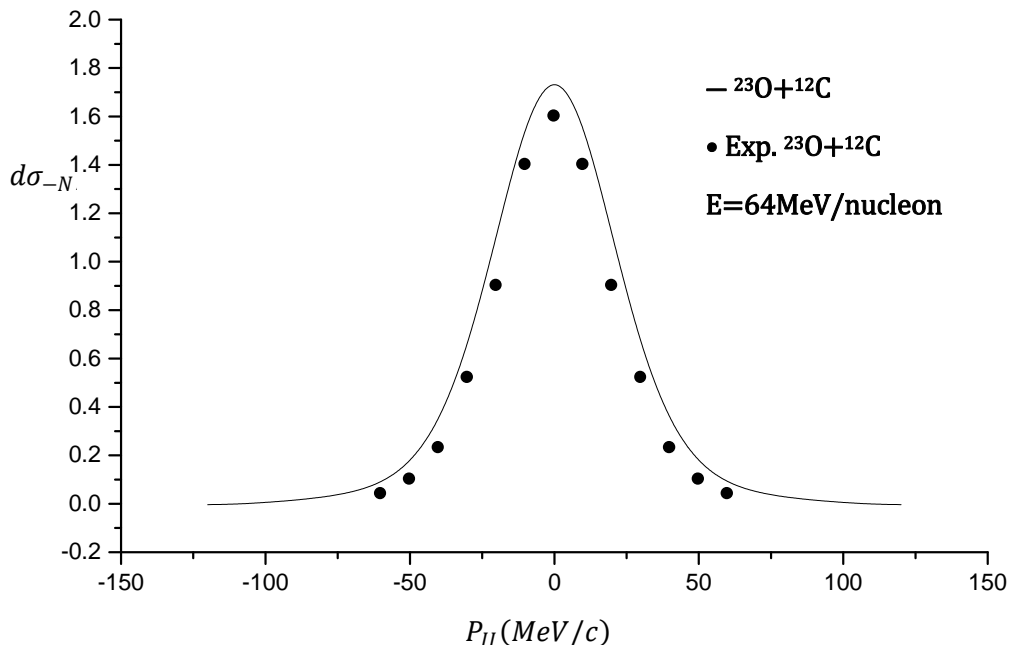


Figure1. Longitudinal Momentum Distribution of the ^{22}O for the reaction $^{23}\text{O}+^{12}\text{C}$ at energy of 64MeV/nucleon. The solid curve denotes the results calculated from Equation (14). The experimental data are taken from (Tostevin et al., 2002).

4.1 Conclusion

The CSC_GM, was modified and used to calculate momentum distributions of the ^{22}O core fragment from $^{23}\text{O}+^{12}\text{C}$ reaction induced by the projectile which has a core plus one valence-neutron. The neutron is in the $1s_{1/2}$ orbit with $n = 1, l = 0, j=0.5$ and the separation energy of $\varepsilon = 0.85$ MeV (Tostevin et al., 2002). However, the narrow momentum distributions of the core nuclei suggest a neutron-halo structure for the ^{22}O structure. The results were compared with available experimental data.

5.0 Acknowledgement

The support of Tertiary Education Trust Fund (TETFund) Nigeria must be duly acknowledged, for immensely supporting this research financially, without which the research would be impossible. The opportunity accorded by the Department of Science Laboratory Technology Kano State Polytechnic to pursue this research to its conclusion must also be acknowledged.

References

- Abu-Ibrahim, B., and Suzuki, Y. (2002). *Calculation of Nucleus-Nucleus Cross sections at Intermediate Energies Using Glauber Theory*. Nuclear physics A 706 (2002) 111-122.
- Adamu, I.D. (2013). *Calculation of Momentum Distributions of ^7Be Fragment from $^8\text{B} + ^{12}\text{C}$ Reaction Using the Glauber Theory*. **IJRRAS** 17(1), 116.
- Basdevant, J.-L., Rich, J., Spiro, M.(2005). *Fundamentals in Nuclear Physics from Nuclear Structure to Cosmology*. XIV, 516P.184 Illus., Hard Cover. ISBN: 978-0-387-01672-6.
- Cortina-Gil, D., Baumann, T., Geissel, H., Lenske, H., Summerer, K., Axelsson, L., Bergmann, U.,Borge, M.J.G., Fraile, L.M., Hellstrom, M., Ivanov, M., Iwasa, N., Janik, R., Jonson, B., Markenroth, K., Munzenberg, G., Nickel, F., Nilsson, T., Ozawa, A., Riisager, K., Schrieder, G., Schwab, W., Simon, H., Scheidenberger, C., Siter, B., Suzuki, T., and Winkler, M.(2001). *One-Nucleon Removal Cross-Sections for $^{17,19}\text{C}$ and $^{8,10}\text{B}$* . The European Physical Journal A-Hadrons and Nuclei, Vol.10, Issue1, pp.49-56.
- Glauber, R.J., Brittin, W.E., and Dunham (Eds.) L.C. (1959). *Lecture on Theoretical Physics*. Interscience, New York. Vol. 1. Pp.315.
- Ogawa, Y., Suzuki, Y. and Tanihata, I. (2003). *Cross Section Calculations in Glauber Model: I. Core Plus One-Nucleon Case*, 151,377. Doi:10.1016/S0010-4655(02)00734-81.
- Ozawa, A., Suzuki, T., and Tanihata, I. (2001). *Nuclear Size and Related Topics*. Nuclear Physics **A69340**. Pp.32-62.
- Salisu, I.S. (2017). *Nuclear Cross-Section Calculations in the Glauber Model*. International Journal of Advanced Academic Research. Vol. 3 (5), pp. 43-50.
- Shukla, A., Sharma, B. K., Chandra, R., Arumugam, P. and Patra, S. K. (2004). *Nuclear Reaction Studies of Unstable Nuclei Using Relativistic Mean Field Formalisms in Conjunction with Glauber Mode.*, APS Journals, 6:21.10.-k, 21.10.dr, 21.30.-x, 24.10.-1, 24.10.Jv.
- Tanihata, I. (1996). *Neutron Halo Nuclei*. *Journal of Physics*. G: Nucl.Part.Phys.Vol.22. Pp.157-198.
- Tostevin, J.A., Bazin, D., Brown, B.A., Glasmacher, T., Hansen, P.G., Madallena, V., Navin, A., and Sherill, B.M. (2002). *Single-Neutron Removal Reactions from ^{15}C and ^{11}Be : Deviations from the Eikonal Approximation*. PhysRevC.66.024607.
- Yi-Bin, W., Yu-Gang, M., Xiang-Zhou, C., Chen, Z., Jin-Gen, C., Hu-Yong, Z., De-Qing, F., Kun, W., Guo-Liang, M., Wei, G., Wen-Dong, T., Wen-Qing, S., Wen-Long, Z., Guo-Qing, X., Hu-Shan, X., Zhi-Yu, S., Jia-Xing. L., Zhong-Yan, G., Meng, W., Zhi-Qiang, C., Zheng-Guo, H., Li-Xin, C., Chen, L., Rui-Shi, M., and Jie, B.(2005). *Parallel Momentum Distribution of ^{28}Si Fragments from ^{29}P* . Chin.Phys.Lett.Vol.22,No.1. Pp.61-64.